

# Compositional Learning for Modular Multi-Agent Self-Organizing Networks

Qi Liao\*, Parijat Bhattacharjee†

\*Nokia Bell Labs, Stuttgart, Germany

†Nokia, Bengaluru, India

E-Mail: \*qi.liao@nokia-bell-labs.com, †parijat.bhattacharjee@nokia.com

**Abstract**—Self-organizing networks face challenges from complex parameter interdependencies and conflicting objectives. This study introduces two compositional learning approaches—Compositional Deep Reinforcement Learning (CDRL) and Compositional Predictive Decision-Making (CPDM)—and evaluates their performance under training time and safety constraints in multi-agent systems. We propose a modular, two-tier framework with cell-level and cell-pair-level agents to manage heterogeneous agent granularities while reducing model complexity. Numerical simulations reveal a 37.2% reduction in handover failures, along with improved throughput and latency, outperforming conventional multi-agent deep reinforcement learning approaches. The approach also demonstrates superior scalability, faster convergence, higher sample efficiency, and safer training in large-scale self-organizing networks.

## I. INTRODUCTION

Self-organizing networks (SON) is a key enabler of autonomous networks, leveraging mechanisms like mobility robustness optimization (MRO) and mobility load balancing (MLB) [1] to dynamically optimize network control parameters using key performance indicators (KPIs). However, its practicality hinges on overcoming challenges such as managing disruptions from inter-function interactions, ensuring scalability for large-scale networks, and implementing robust online safety mechanisms to maintain operational bounds.

Deep learning-based methods have become instrumental in capturing the complexities of multi-objective functions in SON [2]. For example, in [3], a deep learning-based mobility-aware MLB solution was developed, tailoring handover (HO) parameters to specific mobility patterns within individual cells. As networks evolve dynamically, many studies have turned to reinforcement learning for on-the-fly optimization. In [4], the authors aimed at improving cell edge quality of experience (QoE) while optimizing successful handover rates using Q-Learning. To further enhance model accuracy without escalating complexity, multi-agent deep reinforcement learning (MADRL) algorithms are increasingly favored across various use cases. In [5], a coordinated multi-agent deep reinforcement learning algorithm was developed for capacity and QoE optimization, in the context of slicing resource management.

However, the efficacy of conventional MADRL approaches heavily relies on domain-specific characteristics among agents, posing challenges in reproducibility and modularity when deploying solutions across diverse network scenarios and tasks, and often suffering from slow convergence and instability

in large-scale systems. Emerging artificial intelligence (AI) techniques such as compositional learning [6] and modular deep learning [7] are being introduced to address issues of poor model reproducibility and limited sample efficiency.

In this study, we aim to tackle scalability, sample efficiency, and training safety issues in the context of multi-objective SON functions in multi-agent network systems. Our contributions are listed in below.

1) *Two-tier design for heterogeneous agents*: Existing MADRL-based approaches typically define an agent for each cell, focusing on optimizing cell-specific parameters [8]. However, in mobility-related use cases such as MRO and MLB, parameters can be either cell-specific or cell-pair-specific (e.g., specific to cell edges) [9]. These parameters interact strongly, influencing neighboring cells' performance. To address this complexity, we decompose the global problem into two tiers: cell-level agents and cell-pair-level agents, capturing inter-agent dependencies through collaborative observations. To the best of our knowledge, this paper is the first to introduce cell-pair-level agents, with rewards carefully aligned with those of cell-level agents. This design enables a more effective representation of the interdependencies arising from HO events between cell pairs, significantly improving coordination and performance.

2) *Compositional learning and decision making*: Multiple SON objectives are jointly influenced by a common set of features. We first developed the compositional deep reinforcement learning (CDRL) method, which decomposes the reward function into sub-modules, enhancing the model's modularity and reusability while significantly accelerating convergence. However, in real-world systems, CDRL often faces challenges of risky exploration and instability, making it more complex than supervised learning. To address this, we further propose compositional predictive decision-making (CPDM), which optimizes the same objectives as CDRL but is simpler to implement and easier to train. Furthermore, we employed advanced deep learning techniques such as centralized training decentralized execution, order-agnostic sample augmentation, and symlog normalization to improve training performance.

3) *Case study*: We evaluated the performance of the proposed approaches in optimizing multiple SON objectives related to network mobility, capacity, and reliability using a system-level simulator. Compared to the conventional MADRL, our approach exhibited a substantial 37.2% reduction in total handover failures, coupled with enhancements in throughput and reduction in radio link failures, with ensured training

This work was supported by the German Federal Ministry of Education and Research (BMBF) project 6G-ANNA grant 16KIS077K.

safety within the constrained training time. Furthermore, we demonstrate that the proposed CPDM method offers more effective training than CDRL.

The rest of the paper is organized as follows. In Section II, we define the system model and problem formulation. The CDRL and CPDM solutions are described in Section III. In Section IV, we present the case study and the numerical results, and the paper is concluded in Section V.

## II. SYSTEM MODEL AND PROBLEM FORMULATION

We consider a SON system, comprising a set of  $N$  network entities, such as cells, denoted by  $\mathcal{N}$ . Each cell  $n \in \mathcal{N}$  has a set of  $\bar{\mathcal{N}}_n$  neighboring cells, with cardinality  $|\bar{\mathcal{N}}_n| = N_n$ . Let the set of cell pairs associated with cell  $n$  be denoted by  $\mathcal{C}_n := \{(n, m) : m \in \bar{\mathcal{N}}_n\}$ , where  $(n, m)$  represents the cell edge between cells  $n$  and  $m$ , and denote the whole set of cell pairs by  $\mathcal{C}$ . Note that a network entity is not confined to physical cells; it can also encompass virtual entities like network slices or network agents handling groups of users. For detailed information on the parameters and KPIs relevant to SON use cases, we refer readers to [1], and Section IV will explain those pertinent to our case study.

**Control parameters.** There are two types of control parameters: 1) **Cell-level parameters**, such as antenna transmit power, are specific to individual cells. Assuming a number of  $L^{(p)}$  distinct cell-level parameters, denote them as  $\mathbf{p}_n := [p_{n,1}, \dots, p_{n,L^{(p)}}]$  for cell  $n \in \mathcal{N}$ , where  $p_{n,l} \in \mathcal{P}_l$  and  $\mathcal{P}_l$  is the bounded space of the  $l$ -th cell-level parameter. Let  $\mathbf{p} := [\mathbf{p}_1, \dots, \mathbf{p}_N] \in \mathcal{P}$  be the global cell-specific parameters. 2) **Cell pair-level parameters**, often associated with HO behaviors between two neighboring cells, including parameters like cell individual offsets (CIOs) [1]. For a cell pair  $(n, m) \in \mathcal{C}$ , denote the collection of  $L^{(q)}$  parameters as  $\mathbf{q}_{n,m} := [q_{n,m,1}, \dots, q_{n,m,L^{(q)}}]$ , where  $q_{n,m,l} \in \mathcal{Q}_l$ . Here,  $\mathcal{Q}_l$  is the bounded space of the  $l$ -th cell pair-level parameter. Define  $\mathbf{q} := [\mathbf{q}_{n,m} : n \in \mathcal{N}, m \in \bar{\mathcal{N}}_n] \in \mathcal{Q}$  as the global cell pair-level parameters. Note that the cell pair-level parameters are **directional**, meaning  $q_{n,m}$  may not equal  $q_{m,n}$ .

**Observable KPIs.** The Network Operation and Maintenance (O&M) periodically gathers KPIs from all cells, typically averaged over intervals like every 5 to 15 minutes. Similar to control parameters, KPIs can be collected per cell, like cell traffic load or throughput, or per cell pair, including the HO metrics between neighboring cells. Let the **cell-level KPIs** for cell  $n \in \mathcal{N}$  be denoted by  $\boldsymbol{\rho}_n := [\rho_{n,1}, \dots, \rho_{n,L^{(\rho)}}] \in \mathbb{R}^{L^{(\rho)}}$ , and the global cell-level KPIs be  $\boldsymbol{\rho} := [\boldsymbol{\rho}_1, \dots, \boldsymbol{\rho}_N]$ . Denote the **cell pair-level KPIs** for cell pair  $(n, m)$  as  $\boldsymbol{\psi}_{n,m} := [\psi_{n,m,1}, \dots, \psi_{n,m,L^{(\psi)}}] \in \mathbb{R}^{L^{(\psi)}}$ , and the global cell pair-level KPIs as  $\boldsymbol{\psi} := [\boldsymbol{\psi}_{n,m} : (n, m) \in \mathcal{C}] \in \mathbb{R}^{L^{(\psi)} \sum_{n \in \mathcal{N}} N_n}$ .

**Markov decision process.** The system runs on discrete time intervals  $t \in \mathbb{N}_0$ . Considering the network dynamics, we model the multi-cell system as a Markov decision process (MDP) defined by tuple  $\{\mathcal{S}, \mathcal{A}, P(\cdot), r(\cdot), \gamma\}$ , where  $\mathcal{S}$  denotes the state space,  $\mathcal{A}$  is the action space,  $P : \mathcal{S} \times \mathcal{A} \times \mathcal{S} \rightarrow [0, 1]$  indicates the transition dynamics by a conditional distribution that an action in a state leading to a next state, the reward

function is represented by  $r : \mathcal{S} \times \mathcal{A} \rightarrow \mathbb{R}$ , and  $\gamma \in [0, 1]$  is the discount factor.

At time  $t$ , we denote the **global state** as  $\mathbf{s}(t) := [\boldsymbol{\rho}(t), \boldsymbol{\psi}(t)] \in \mathcal{S} := \mathbb{R}^{NL^{(\rho)}L^{(\psi)} \sum_{n \in \mathcal{N}} N_n}$ , as an observation of the entire system consisting of both cell-level and cell pair-level KPIs. The **global action** is denoted by  $\mathbf{a}(t) := [\mathbf{p}(t), \mathbf{q}(t)] \in \mathcal{A} := \mathcal{P} \times \mathcal{Q}$ . The **global reward**  $r(t) \in \mathbb{R}$ , dependent on  $(\mathbf{s}(t), \mathbf{a}(t))$ , is a scalar computed from the collected KPIs  $\boldsymbol{\rho}(t+1)$  and  $\boldsymbol{\psi}(t+1)$ .

In line with the classical reinforcement formulation, the global problem is finding the policy  $\pi : \mathcal{S} \rightarrow \mathcal{A}$  for optimizing the control parameters based on the KPI observations, to maximize the expected cumulative discounted reward of a trajectory for a finite time horizon  $T$ :

$$\max_{\pi} \mathbb{E}_{\pi} \left[ \sum_{t=0}^T \gamma^t r(\mathbf{s}(t), \mathbf{a}(t)) \right], \text{ s.t. } \mathbf{a}(t) \in \mathcal{A}. \quad (1)$$

Given the vast state and action space, the global problem is intractable. Therefore, we seek distributed and efficient solutions with online safety assurance.

## III. COMPOSITIONAL LEARNING AND DECISION-MAKING

In this section, we propose a novel distributed compositional learning and decision-making approach to accelerate learning and guarantee training safety. The two key enablers are: 1) *two-tier modular design for heterogeneous agents*, and 2) *compositional learning of the value function*.

### A. Two-Tier Modular Design for Heterogeneous Agents

We are interested in decomposing the global agent into local ones for efficient and highly scalable distributed implementation. Many works have proposed constructing per-cell agents to optimize cell-level parameters  $\mathbf{p}_n$  based on local observations  $\boldsymbol{\rho}_n$  and possibly exchanged observations [5]. However, when considering cell pair-level parameters and KPIs, the challenge arises from both strong inter-cell dependencies and **varying number of neighboring cells** each cell may have, leading to different state and action dimensions across cells. This requires local agents to adjust their model size according to the number of neighboring cells, with limited model reusability.

We propose a two-tier approach, comprising the first-tier cell-level agents (CAs) and the second-tier cell pair-level agents (CPAs), each with fixed input and output dimensions universally applicable across different cells and cell pairs, as shown in Figure 1. We adopt the widely used *centralized training with decentralized execution (CTDE)* approach [10], allowing local samples from different cells to contribute to training a shared model that captures general behaviors across various cells. Then, during the inference phase, the trained model can be loaded and executed distributedly. Note that CAs and CPAs do not have to be deployed at their respective cells, but anywhere in a virtual server.

1) *Cell-Level Agents:* At time  $t$ , the **action** of the CA in the  $n$ -th cell is  $\mathbf{a}_n(t) := \mathbf{p}_n(t)$ . The **state** is defined as  $\mathbf{s}_n(t) := [\boldsymbol{\rho}_n(t), \mathbf{g}_0(\boldsymbol{\psi}_n(t))]$ , where  $\mathbf{g}_0$  is a mapping from  $L^{(\psi)} N_n$  cell pair KPIs (varying dimensions for each  $n \in \mathcal{N}$ ) to

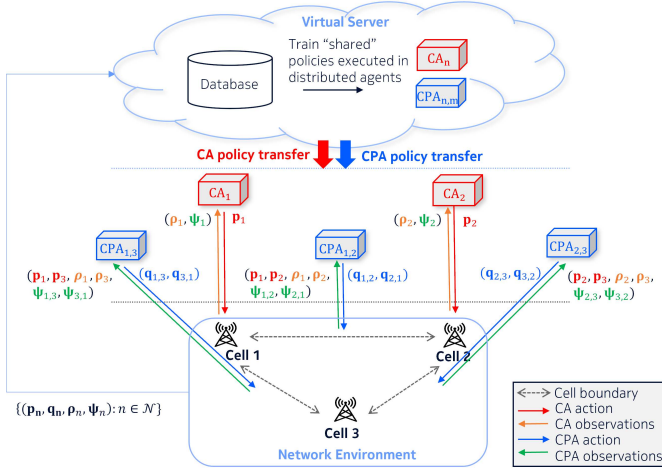


Figure 1: CTDE-based two-tier agents.

a reduced fixed dimension of features. For instance, an efficient and practical solution is to simply compute the mean of each cell pair KPI over cell pairs  $\mathcal{C}_n$  [5]:

$$\mathbf{g}_0 : \mathbb{R}^{L(\psi)N_n} \rightarrow \mathbb{R}^{L(\psi)} : \psi_n \mapsto \left[ \bar{\psi}_{n,l} : l = 1, \dots, L(\psi) \right] \quad (2)$$

where  $\bar{\psi}_{n,l} := \frac{1}{N_n} \sum_{m \in \bar{N}_n} \psi_{n,m,l}$ .

Let the action and state spaces of any CA be denoted by  $\mathcal{A}^{(C)}$  and  $\mathcal{S}^{(C)}$ , respectively. We have  $\mathcal{A}^{(C)} := \prod_{l=1}^{L(p)} \mathcal{P}_l$  and  $\mathcal{S}^{(C)} := \mathbb{R}^{L(\rho)+L(\psi)}$ , with fixed action and state dimensions for any  $n \in \mathcal{N}$ , regardless of  $N_n$ .

The multi-objective **reward** captures both cell KPIs  $\rho_n$  and cell pair KPIs  $\psi_n$ . Detail definitions will be provided in Section IV-A for the case study. Here we give a general formulation:

$$r_n(t) = w_1 g_1(\rho_n(t+1)) + w_2 \frac{1}{N_n} \sum_{m \in \bar{N}_n} g_2(\psi_{n,m}(t+1), \psi_{m,n}(t+1)), \quad (3)$$

where  $g_1 : \mathbb{R}^{L(\rho)} \rightarrow \mathbb{R}$  and  $g_2 : \mathbb{R}^{2L(\psi)} \rightarrow \mathbb{R}$ , and  $w_1$  and  $w_2$  are the weight factors balancing cell KPIs and cell pair KPIs.

2) *Order-Agnostic Cell Pair-Level Agents*: The action of the CPA for cell pair  $(n, m)$  is  $\bar{\mathbf{a}}_{n,m}(t) := [\mathbf{a}_{n,m}(t), \mathbf{a}_{m,n}(t)] \in \mathcal{A}^{(CP)} := \prod_{l=1}^{L(a)} \mathcal{Q}_l^2$ . We allow the CPA to observe both its cell pair KPIs and its belonging cell's KPIs. In addition, we include the cell parameters  $\mathbf{p}_n$  in the observation space, as the first-tier CAs make the decision first. Thus, we have  $\bar{\mathbf{s}}_{n,m}(t) := [\mathbf{p}_n(t), \mathbf{p}_m(t), \rho_n(t), \rho_m(t), \psi_{n,m}(t), \psi_{m,n}(t)]$ . The state space yields  $\mathcal{S}^{(CP)} := \prod_{l=1}^{L(p)} \mathcal{P}_l^2 \times \mathbb{R}^{4L(\rho)+L(\psi)}$ , and the state has a fixed dimension of  $2(L(p) + L(\rho) + L(\psi))$ . We further compute the reward with the same mapping  $g_1$  and  $g_2$ :

$$\bar{r}_{n,m}(t) = w_1 g_1(\rho_n(t+1)) + w_2 g_2(\psi_{n,m}(t+1), \psi_{m,n}(t+1)). \quad (4)$$

**Remark 1** (Aligned reward of CAs and CPAs). From (3) and (4), we have  $r_n(t) = (1/N_n) \cdot \sum_{m \in \bar{N}_n} \bar{r}_{n,m}(t)$ . Thus, improving the rewards of CPAs associated to cell  $n$  also improves the reward of the CA of cell  $n$ .

**Remark 2** (Order-agnostic training). A CPA should represent the joint behavior of both cell boundaries ( $n \rightarrow m$  and  $m \rightarrow n$ ) within an order-agnostic cell tuple  $(n, m)$ . For example, for cell pair  $(1, 2)$ , it should not matter whether  $n = 1, m = 2$  or  $n = 2, m = 1$ . Therefore, to ensure CPAs adaptable to arbitrary orders, we augment collected sample sets, including in the replay buffer both samples:  $(\bar{\mathbf{s}}_{n,m}(t), \bar{\mathbf{a}}_{n,m}(t), \bar{r}_{n,m}(t), \bar{\mathbf{s}}_{n,m}(t+1))$  and  $(\bar{\mathbf{s}}_{m,n}(t), \bar{\mathbf{a}}_{m,n}(t), \bar{r}_{m,n}(t), \bar{\mathbf{s}}_{m,n}(t+1))$ .

Compared to the conventional per-cell agents that integrate all cell pair parameters and KPIs into action and state spaces, our two-tier approach achieves much lower complexity and greater modularity, while aligning the objectives of CAs and CPAs. Table I compares the dimensions of our proposed two-tier agents with conventional per-cell agents that include  $\mathbf{q}_n$  in action and  $\{(\psi_{n,m}, \psi_{m,n}) : m \in \bar{N}_n\}$  in states.

## B. Actor-Critic Algorithm and Alternating Direction Method

With the defined states, actions, and rewards, the two-tier CAs and CPAs search for the policies  $\pi_n : \mathcal{S}^{(C)} \rightarrow \mathcal{A}^{(C)}, \forall n \in \mathcal{N}$  and  $\bar{\pi}_{n,m} : \mathcal{S}^{(CP)} \rightarrow \mathcal{A}^{(CP)}, \forall (n, m) \in \mathcal{C}$ , respectively, by jointly solving the following CA and CPA problems:

$$\max_{\pi_n : \mathbf{a}_n \in \mathcal{A}^{(C)}} \mathbb{E}_{\pi_n} \left[ \sum_{t=0}^T \gamma^t r_n(\mathbf{s}_n(t), \mathbf{a}_n(t)) \right], \quad (5)$$

$$\max_{\bar{\pi}_{n,m} : \bar{\mathbf{a}}_{n,m} \in \mathcal{A}^{(CP)}} \mathbb{E}_{\bar{\pi}_{n,m}} \left[ \sum_{t=0}^T \gamma^t \bar{r}_{n,m}(\bar{\mathbf{s}}_{n,m}(t), \bar{\mathbf{a}}_{n,m}(t)) \right]. \quad (6)$$

1) *Actor-Critic Algorithms*: In subsequent subsections, for brevity, we refer to the state and action at time  $t$  as  $\mathbf{s}_t, \mathbf{a}_t$  respectively, while  $r, \pi$  represent the reward and policy, respectively, regardless of CA or CPA. We choose actor-critic methods [11] to solve deep reinforcement learning (DRL) problems, for its effectiveness when dealing with high dimensional spaces. Such methods learn a critic function  $Q(\mathbf{s}_t, \mathbf{a}_t | \theta)$ , typically a multi-layer perceptron (MLP) parameterized by  $\theta$ , to approximate the value function  $Q^\pi(\mathbf{s}_t, \mathbf{a}_t)$ , which describes the expected return after taking an action  $\mathbf{a}_t$  in state  $\mathbf{s}_t$  following policy  $\pi$ . In addition, an actor  $\pi(\mathbf{s}_t | \phi)$  parameterized by  $\phi$  updates the action  $\mathbf{a}_t$  based on observation  $\mathbf{s}_t$ . In this paper, we consider the widely used Twin Delayed Deep Deterministic policy gradient (TD3) [12]. The action is updated by policy gradient based on the expected cumulative reward  $J$  with respect to the actor parameter  $\phi$ , as:

$$\nabla_{\phi} J \approx \mathbb{E} [\nabla_{\mathbf{a}} Q(\mathbf{s}, \mathbf{a} | \theta) |_{\mathbf{s}=\mathbf{s}_t, \mathbf{a}=\pi(\mathbf{s}_t)} \nabla_{\phi} \pi(\mathbf{s}_t | \phi)]. \quad (7)$$

The critic parameter  $\theta$  is updated by minimizing the loss of temporal difference (TD), given by:

$$L_t(\theta) = \mathbb{E} [(g_t - Q(\mathbf{s}_t, \mathbf{a}_t | \theta))^2], \quad (8)$$

where  $g_t = r_t + \gamma Q(\mathbf{s}_{t+1}, \pi(\mathbf{s}_{t+1} | \phi) | \theta)$ .

2) *Joint CA and CPA Training with Alternating Direction*: The classical actor-critic methods can solve the local problems in CAs and CPAs if they operate independently. However, the rewards in CA and CPA are jointly influenced by cell-level and cell pair-level actions. To address this interaction, one potential

Table I: Comparison among the agents and their dimensions.

	Conventional neighbor-aware per-cell agent	Our proposed two-tier agents	
		CA	CPA
Action	$\mathbf{a}'_n := [\mathbf{p}_n, \mathbf{q}_n]$	$\mathbf{a}_n := \mathbf{p}_n$	$\bar{\mathbf{a}}_{n,m} = [\mathbf{q}_{n,m}, \mathbf{q}_{m,n}]$
Action dim.	$L^{(\mathbf{p})} + N_n \cdot L^{(\mathbf{q})}$	$L^{(\mathbf{p})}$	$2L^{(\mathbf{q})}$
State	$\mathbf{s}'_n := [\rho_n, (\psi_{n,m}, \psi_{m,n}) : m \in \mathcal{N}_n]$	$\mathbf{s}_n := [\rho_n, \mathbf{g}_0(\psi_n)]$	$\bar{\mathbf{s}}_{n,m} := [\mathbf{p}_n, \mathbf{p}_m, \rho_n, \rho_m, \psi_{n,m}, \psi_{m,n}]$
State dim.	$L^{(\rho)} + 2N_n L^{(\psi)}$	$L^{(\rho)} + L^{(\psi)}$	$2(L^{(\mathbf{p})} + L^{(\rho)} + L^{(\psi)})$
Reward	$r_n \in \mathbb{R}$ in (3)	$r_n \in \mathbb{R}$ in (3)	$\bar{r}_{n,m} \in \mathbb{R}$ in (4)

approach is to employ alternating direction methods, which iteratively update different sets of parameters, while holding others fixed. In the context of training CAs and CPA, this involves alternating between updating the actors and critics in CAs and the actors and critics in CPAs, as well as alternating the actions  $\mathbf{a}_n$  and  $\bar{\mathbf{a}}_{n,m}$ . Because the objectives of CAs and CPAs are aligned (Remark 1), doing this allows for addressing the interplay between these two levels of automata. Additionally, given the broader impact of CA decisions on associated cell pairs, we use a lower update frequency for CAs compared to CPAs to promote stability during training and reduce the risk of over-fitting. Note that although alternating direction method of multipliers (ADMM) exhibits good performance for convex problems [13], its convergence in deep learning remains intriguing. Empirical evidence suggests that they can converge effectively in deep learning [14]. In this paper, we only provide empirical studies to show its effectiveness in joint training of CAs and CPAs.

### C. CDRL: Compositional Deep Reinforcement Learning

The above-introduced actor-critic algorithms often face challenges of slow convergence, especially with complex, multi-objective reward functions. Considering that SON multi-objectives are composed of different aspects of the performance, e.g., enhancing throughput, reducing delay and HO failures, we propose to decompose the critic into multiple sub-critics, each responsible for evaluating a different objective. By breaking down the value function into smaller, more specialized components, we can enhance the modularity, interpretability, and hierarchical representation of the DRL model. As shown in Figure 2, the value function to estimate  $v^\pi(s)$  is decomposed to  $K$  prediction functions of the sub-critics  $\{\mathbf{h}_1, \dots, \mathbf{h}_K\}$ , with parameters  $\{\theta_1, \dots, \theta_K\}$ , providing predicted metrics  $\{\omega_1, \dots, \omega_K\}$  respectively. Then, a task aggregator  $f$ , e.g., an MLP with parameters  $\theta_0$ , returns the Q value based on the predicted metrics. The loss of the critic includes both the TD error and the prediction loss:

$$\begin{aligned} \tilde{L}_t(\theta_0, \theta_1, \dots, \theta_K) := & L_t(\theta_0, \theta_1, \dots, \theta_K) + \\ & \frac{1}{K} \sum_{k=1}^K \|\mathbf{h}_k(\mathbf{s}_t, \mathbf{a}_t | \theta_k) - \hat{\omega}_{k,t+1}\|_2, \end{aligned} \quad (9)$$

where  $L_t$  is the classical TD loss at time  $t$  of TD3 algorithm,  $\hat{\omega}_{k,t+1}$  is the actual measured  $k$ -th metrics at time  $t+1$ .

**Remark 3** (Symlog normalization). *The scale of the network parameters and KPIs can vary significantly between domains. Predicting large targets using a squared loss function may result in divergence, while absolute and Huber losses might*

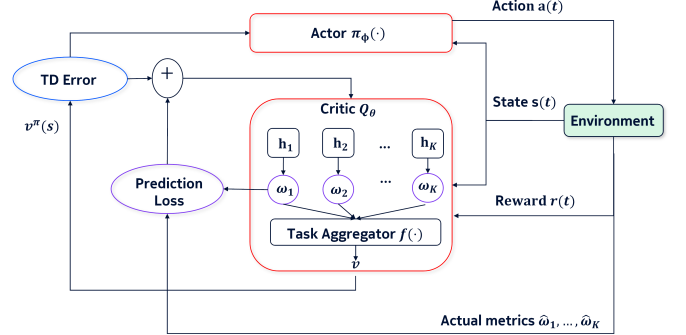


Figure 2: Basic architecture of CDRL.

*impede learning progress. To address the dilemma, we use symlog normalization and apply a function selected from the bi-symmetric logarithmic family:  $\text{symlog}(x) := \text{sign}(x) \ln(|x| + 1)$ . To read out the prediction and compute the loss function of the prediction, the inverse transformation is  $\text{symexp}(x) := \text{sign}(x)(\exp(|x|) - 1)$ .*

### D. CPDM: Compositional Predictive Decision-Making

Despite the benefits of the proposed two-tier mechanism and compositional learning, challenges persist in balancing exploration and exploitation in DRL approaches. The exploration phase often results in hazardous outcomes during training. In real-life scenarios, predictive decision-making approaches may offer advantages of safety guarantees compared to DRL algorithms [15].

The proposed CPDM approach modifies the action space by optimizing the step size of increasing or decreasing control parameters. Specifically, for cell-level parameters we have  $\mathbf{a}_n(t) = \mathbf{p}_n(t+1) - \mathbf{p}_n(t) \in \Delta\mathcal{A}^{(C)}$  for  $n \in \mathcal{N}$ , and for cell pair-level parameters  $\bar{\mathbf{a}}_{n,m}(t) = \mathbf{q}_{n,m}(t+1) - \mathbf{q}_{n,m}(t) \in \Delta\mathcal{A}^{(CP)}$ ,  $\forall (n,m) \in \mathcal{C}$ . In practical implementations, the change in action at each step is restricted to ensure the stability of the system. Consequently,  $\Delta\mathcal{A}^{(C)}$  and  $\Delta\mathcal{A}^{(CP)}$  are significantly smaller than  $\mathcal{A}^{(C)}$  and  $\mathcal{A}^{(CP)}$ .

With the reduced action space, we have the ability to exhaustively compute the predicted value function for all potential changes within the constrained action space, and select the one with the maximum predicted value:

$$\mathbf{a}_n^* = \arg \max_{\mathbf{a}_n \in \Delta\mathcal{A}^{(C)}} f^{(C)}(\mathbf{s}_n, \mathbf{a}_n), \quad (10)$$

$$\bar{\mathbf{a}}_{n,m}^* = \arg \max_{\bar{\mathbf{a}}_{n,m} \in \Delta\mathcal{A}^{(CP)}} f^{(CP)}(\bar{\mathbf{s}}_{n,m}, \bar{\mathbf{a}}_{n,m}), \quad (11)$$

where  $f^{(C)}$  and  $f^{(CP)}$  are the aggregator functions of CA and CPA respectively. This exhaustive search approach is facilitated by modern deep learning frameworks, which efficiently inference large batches of input samples.

#### IV. CASE STUDY AND PERFORMANCE EVALUATION

We apply the proposed CDRL and CPDM approaches to SON use cases, targeting multi-objective optimization to enhance HO performance, throughput, and latency while reducing radio link failures (RLFs) by tuning mobility parameters such as time-to-trigger (TTT) and CIO.

##### A. Case Study

With a slight abuse of notation, for CA  $n$ , we define a cell-level parameter TTT  $p_n$  within the space  $\mathcal{P} := \{40, 64, 80, 100, 128, 160, 256, 320, 480, 512, 640, 1024, 1280, 2560, 5120\}$  in ms. For CPA  $(n, m)$ , the cell pair-level parameters CIOs are  $q_{n,m}, q_{m,n} \in \mathcal{Q} := \{-24, -23, \dots, 24\}$  in dB [16]. Namely, we deal with the case where  $L^{(p)} = L^{(q)} = 1$ .

Although TTT and CIO are mobility-related parameters, they jointly affect various KPIs including HO KPIs, cell load, throughput, and latency. This is because a user served by cell  $n$  will undergo handover to the neighboring cell  $m \in \bar{\mathcal{N}}_n$  if the following criterion holds [16]:

$$\text{RSRP}_m > \text{RSRP}_n + q_{n,m} \text{ holds for } p_n \text{ ms,} \quad (12)$$

where  $\text{RSRP}_i$  is the reference signal received power (RSRP) from cell  $i$ . Conversely, similar conditions apply for handover from cell  $m$  to cell  $n$ . Thus, large values of them may lead to too-late handover (**HOL**), potentially resulting in RLF before the handover completes. In contrast, small values may cause too-early handover (**HOE**), where a handover occurs before the neighboring cell can provide a sustainable signal quality, leading to a RLF right after the handover. Another event due to the early HO decisions is the wrong-cell handover (**HOW**). Also, inappropriate settings of  $q_{n,m}$  and  $q_{m,n}$  lead to frequent handovers between cells, commonly known as ping-pong handover (**HOPP**). Moreover, the handover behavior directly influences load distribution across cells, thereby substantially affecting cell throughput and latency.

**Two-tier actions.** When applying CDRL, because TD3 works with continuous action space, the actions of CA  $n$  and CPA  $(n, m)$  are defined as  $a_n := p_n \in \mathcal{A}^{(C)} := [40, 5120]$  and  $\bar{a}_{n,m} := [q_{n,m}, q_{m,n}] \in \mathcal{A}^{(CP)} := [-24, 24]^2$ , respectively. Then, we choose the nearest values to the actors' outputs in the defined sets  $\mathcal{P}$  and  $\mathcal{Q}$  to execute. On the other hand, for CPDM, we have different search space  $\Delta\mathcal{A}^{(C)}(p_n(t))$ , depending on the current TTT value  $p_n(t)$ , because the values in  $\mathcal{P}$  are not uniformly distributed. It computes the difference from the five values, spanning from the two on the left to the two on the right of  $p_n(t)$  within the set  $\mathcal{P}$ , and  $\Delta\mathcal{A}^{(CP)} := \{-2, -1, 0, 1, 2\}^2$  in dB. Thus, we can search the whole discrete action space, and the size of the search space for each CA is only 5, and for each CPA is 25. The cell pair actions  $\bar{a}_{n,m}$  are updated every 15 minutes, while the update frequency of  $a_n$  is slower, for every hour, allowing for more stable adjustments to cell-level parameters.

**Partial-observable states.** The states for both CDRL and CPDM are defined in the same way as presented in Table I. The following 7 cell-level KPIs are included in  $\rho_n$  for each CA  $n$ : downlink average user throughput, uplink average user

throughput, downlink physical resource block (PRB) usage, uplink PRB usage, number of active users, number of RLFs, and average channel quality indicator (CQI). The cell pair-level KPIs  $\psi_{n,m}$  include the number of HO attempts, HO success ratio, and the numbers of HOLs, HOEs, HOWs, and HOPPs.

**Multi-objective rewards.** The multi-objective reward is constructed based on the following three prediction functions: 1) The **HO prediction** function  $h_1(\cdot)$  is designed to predict HO cost, defined as  $C^{(\text{HO})} = \alpha_0 R^{(\text{HOL})} - \alpha_1 R^{(\text{HOE})} - \alpha_2 R^{(\text{HOW})} - \alpha_3 R^{(\text{HOPP})}$ , where  $\alpha_i, i = 0, \dots, 3$  are positive weights in the range  $[0, 1]$ , and  $R^{(\text{HOL})}, R^{(\text{HOE})}, R^{(\text{HOW})}, R^{(\text{HOPP})}$  represent the ratios of HO events (HOL, HOE, HOW, and HOPP) to the total number of HO attempts, respectively, typically set to 1, 1, 1, 0.2. Since these ratios cannot exceed 1, the HO cost is in the range  $[0, 1]$ . A large positive HO cost indicates too-late HO decisions, while a large negative value indicates too-early HO decisions. Ideally,  $C^{(\text{HO})}$  should approach 0, indicating a balanced HO decision strategy with a good trade-off between too-early and too-late HO behaviors.

2) The **throughput and latency classification** function  $h_2(\cdot)$  is designed to predict the quantified class of throughput and latency, with three predefined classes "good", "normal", "poor". This classification approach is chosen over predicting exact values because throughput and latency are influenced by dynamic user traffic patterns, and a low throughput during peak hours may not necessarily indicate poor performance. The labels for these classes are computed based on the time-dependent distribution of throughput and latency observations. This involves analyzing historical data to determine the typical range of throughput and latency values observed at different times of the day and define the thresholds to classify them into the appropriate class.

3) The **RLF anomaly prediction** function  $h_3(\cdot)$  is a binary classifier to predict the anomaly increase of RLF events. This choice of a binary classifier is motivated by the need to exclude RLF caused by other network issues, such as poor coverage. Similar to the throughput and latency classifier, the labels are computed based on historical data analysis.

To incorporate the HO cost, throughput and latency classification, and RLF anomaly prediction into rewards (3) and (4), we define auxiliary functions  $g_1(\cdot)$  and  $g_2(\cdot)$  as follows.  $g_1(\cdot)$  computes  $1 - |C^{(\text{HO})}|$ , ensuring it lies in the range  $[0, 1]$ .  $g_2(\cdot)$  computes  $\mathbb{1}_{\{\hat{h}_2 = \text{'good'}\}} + 0.5 \cdot \mathbb{1}_{\{\hat{h}_2 = \text{'normal'}\}} + \mathbb{1}_{\{\hat{h}_3 = \text{'normal'}\}}$  where  $\mathbb{1}_{\{X\}}$  is the indicator function equals 1 if event  $X$  occurs. Thus, the CA and CPA rewards are both upper-bounded by 3.

##### B. Numerical Results

We evaluate the proposed CDRL and CPDM approaches using a self-developed system-level simulator mimicking a real-world scenario. The radio map is extracted from a part of Helsinki, including 12 sites with 32 cells operating in the 2.4 GHz frequency band as depicted in Figure 3. The user's mobility is generated with the SUMO traffic simulator [17]. The number of users in the simulated area follows a realistic daily pattern based on real data. The agent interacts with the simulator with a granularity of simulation slots 900,

Table II: KPI comparison with 14-day trial.

	DL throughput in Mbps	DL latency in ms	HOLR in %	HOER in %	HOWR in %	HOPPR in %	Throughput anomaly in %	RLF anomaly in %
DFLT	29.62	6.13	0.93	0.43	0.39	21.23	N/A	N/A
MADRL	28.61	<b>5.81</b>	1.22	0.36	0.46	<b>16.37</b>	28.84	0.63
H-MADRL	29.23	6.02	0.88	0.38	0.41	17.56	16.95	0.35
CDRL	30.05	5.95	0.72	0.31	0.38	18.10	12.48	0.28
CPDM	<b>30.14</b>	5.90	<b>0.62</b>	<b>0.30</b>	<b>0.36</b>	17.37	<b>6.26</b>	<b>0.02</b>



Figure 3: Simulated network scenario with 10 three-sector sites and 2 one-sector sites in Helsinki.

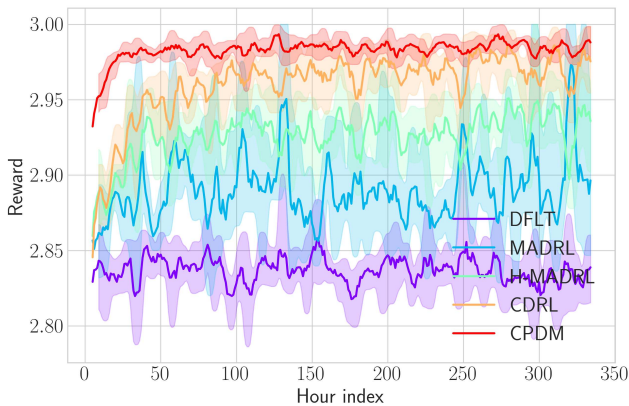


Figure 4: Performance comparison: Reward evolution during training, reflecting 15-minute intervals of real-life time. This allows for 96 interactions per day. A total of 12 days of training and 2 days of evaluation are conducted, that is, with a maximum hour index of 336.

1) *Training Parameters*: As for the neural network architecture, for both CAs and CPAs, MLPs are used for the actor network, with 3 hidden layers. The number of neurons for each layer is set to (64, 32, 8). Additionally, each compositional critic predictor is implemented as an MLP with 3 hidden layers, having (32, 16, 8) neurons. The symlog normalization described in Remark 3 is applied to both inputs and outputs. The learning rates of the actor and critic are 0.001 and 0.002, respectively. The batch size is 64, and the Adam optimizer is employed.

2) *Methods to Comparison*: We compare the performance of the following five methods:

- **DFLT**: Default setting where all TTTs values are set to 320 ms and CIOs values are set to 0 dB.

- **MADRL**: The conventional baseline neighbor-aware per-cell agent scheme using DRL as introduced in Table I.
- **H-MADRL**: MADRL with the two-tier heterogeneous agents introduced in Section III-A, but without compositional learning.
- **CDRL**: MADRL with both two-tier heterogeneous agents and compositional learning proposed in Section III-C.
- **CPDM**: The two-tier agent scheme using compositional predictive optimization, proposed in Section III-D.

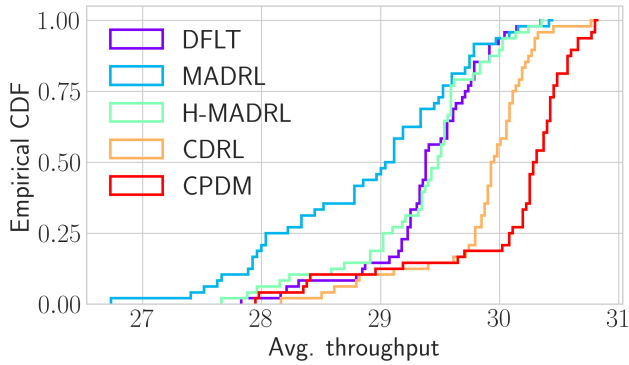
3) *Training Performance*: In Figure 4, we compare the reward evolution of the five methods discussed. It is evident that MADRL struggles to converge within the constrained training timeframe. H-MADRL shows a slight improvement over MADRL by leveraging its two-tier modular light models. When both the two-tier design of heterogeneous agents and compositional learning are applied, CDRL achieves a further acceleration in the convergence speed.

However, due to the limited sample size, the DRL-based approaches still fail to converge within the given training period. This is likely attributed to the joint training of actor and critic networks, which can introduce instability and demand longer training durations for effective convergence. In contrast, CPDM significantly outperforms all DRL-based methods. Its superior performance stems from the efficient learning facilitated by lightweight prediction models and robust prediction-based decision-making.

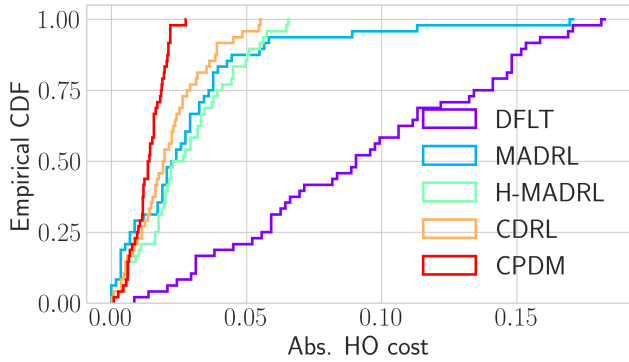
4) *Inference Performance*: Table II presents a comparison of the averaged KPIs over the evaluation period. Throughput and RLF anomalies are identified by analyzing performance deviations from the default configuration for each hour of the day and each cell. Consequently, these values are marked as N/A for DFLT. The baseline cell-based MADRL approach shows unsatisfactory performance, likely due to its complexity, which hinders full convergence. It often over-corrects too-early HO behaviors, leading to an increase in RLF and HOL events. Note that the lowest latency observed for MADRL may result from excessive user dropping.

Figure 5 depicts the empirical cumulative distribution functions (CDFs) of average throughput and absolute HO cost. Notably, a HO cost approaching 0 reflects an effective trade-off in HO behavior, balancing between too-late and too-early HOs.

Ultimately, compared to the default configuration, CPDM achieves a 33.3% reduction of too-late HOs and 30.2% reduction of too-early HOs, with slight improvement in throughput and latency. Compared with CDRL, CPDM significantly reduces the throughput and RLF anomalies.



(a) CDF of average throughput.



(b) CDF of absolute HO cost.

Figure 5: Performance comparison of CDFs.

5) *Accuracy of Compositional Predictive Functions:* The compositional learning of the prediction functions achieves accurate prediction results, with 0.006 mean absolute error on HO cost, 86.8% precision and 81.1% recall on throughput classification, and 94.6% precision and 92.0% recall on RLF anomaly detection (plots omitted due to the limited space).

6) *Key Takeaways:* We summarized the takeaways from the numerical results as follows:

- Due to practical limitations in learning time, the MADRL baseline approach fails to achieve convergence. The proposed two-tier agent design, featuring cooperating CAs and CPAs, effectively improves learning speed. In addition, compositional learning of the reward function further accelerates convergence.
- Under limited sample availability, predictive decision-making approaches exhibit greater stability and effectiveness compared to DRL-based methods. The proposed two-tier heterogeneous agent framework, combined with compositional learning, significantly reduces model complexity, enhances collaborative capabilities, and improves model reusability across different SON objectives.

## V. CONCLUSION

This paper studies multi-agent SON network systems, seeking to alleviate complexities and bolster modularity through the exploration of two compositional learning methods: CDRL

and CPDM. By leveraging a modular framework comprising two-tier distributed agents, we effectively mitigate model complexity while enhancing knowledge transferability. The numerical assessments demonstrate the remarkable efficacy of our approach, particularly in terms of sample efficiency, convergence rate, and training safety. These findings suggest that prediction-based decision-making methods may present a more stable and effective performance than the DRL methods in industrial applications with costly training periods.

## REFERENCES

- [1] 3GPP, *TS 32.500: Self-Organizing Networks (SON); Concepts and requirements; Rel-17*, 3GPP Technical specification (TS), 2022.
- [2] A. Banerjee, S. S. Mwanje, and G. Carle, "Trust and performance in future AI-enabled, open, multi-vendor network management automation," *IEEE Transactions on Network and Service Management*, vol. 20, no. 2, pp. 995–1007, 2023.
- [3] A. Mohajer, M. Bavaghar, and H. Farrokhi, "Mobility-aware load balancing for reliable self-organization networks: Multi-agent deep reinforcement learning," *Reliability Engineering & System Safety*, vol. 202, p. 107056, 2020.
- [4] M. L. Marf-Altozano, S. S. Mwanje, S. L. Ramírez, M. Toril, H. Sanneck, and C. Gijón, "A service-centric Q-learning algorithm for mobility robustness optimization in LTE," *IEEE Transactions on Network and Service Management*, vol. 18, no. 3, pp. 3541–3555, 2021.
- [5] T. Hu, Q. Liao, Q. Liu, D. Wellington, and G. Carle, "Inter-cell slicing resource partitioning via coordinated multi-agent deep reinforcement learning," in *IEEE ICC*, 2022.
- [6] S. Purushwalkam, M. Nickel, A. Gupta, and M. Ranzato, "Task-driven modular networks for zero-shot compositional learning," in *IEEE/CVF ICCV*, 2019, pp. 3593–3602.
- [7] J. Pfeiffer, S. Ruder, I. Vulić, and E. M. Ponti, "Modular deep learning," *arXiv preprint arXiv:2302.11529*, 2023.
- [8] A. Feriani and E. Hossain, "Single and multi-agent deep reinforcement learning for AI-enabled wireless networks: A tutorial," *IEEE Communications Surveys & Tutorials*, vol. 23, no. 2, pp. 1226–1252, 2021.
- [9] Q. Liao, T. Hu, and D. Wellington, "Knowledge transfer in deep reinforcement learning for slice-aware mobility robustness optimization," in *IEEE ICC*, 2022, pp. 4262–4268.
- [10] R. Lowe *et al.*, "Multi-agent actor-critic for mixed cooperative-competitive environments," *Advances in neural information processing systems*, vol. 30, 2017.
- [11] V. Konda and J. Tsitsiklis, "Actor-Critic algorithms," in *NIPS*, 1999.
- [12] S. Fujimoto *et al.*, "Addressing function approximation error in Actor-Critic methods," *ArXiv*, vol. abs/1802.09477, 2018.
- [13] S. P. Boyd and L. Vandenberghe, *Convex optimization*. Cambridge university press, 2004.
- [14] J. Zeng, S.-B. Lin, Y. Yao, and D.-X. Zhou, "On ADMM in deep learning: Convergence and saturation-avoidance," *Journal of Machine Learning Research*, vol. 22, no. 199, pp. 1–67, 2021.
- [15] T. Hu, Q. Liao, Q. Liu, A. Massaro, and G. Carle, "Fast and scalable network slicing by integrating deep learning with Lagrangian methods," in *GLOBECOM*. IEEE, 2023, pp. 6346–6351.
- [16] 3GPP, *Radio Resource Control (RRC) protocol specification; Rel-18*, 3GPP Technical specification (TS), 2024.
- [17] P. A. Lopez *et al.*, "Microscopic traffic simulation using SUMO," in *ITEC*. IEEE, 2018. [Online]. Available: <https://elib.dlr.de/124092/>